Proceedings of the XVII ECSMGE-2019
Geotechnical Engineering foundation of the future
ISBN 978-9935-9436-1-3

doi: 10.32075/17ECSMGE-2019-0206

XVII European Conference
ECSMGE 2019
Reykjavik
on Soil Mechanics
and Geotechnical Engineering

Centrifuge modelling of a pile group foundation in a multilayered soil under sinusoidal and seismic loadings

Modélisation en centrifugeuse d'un groupe de pieux dans un sol multicouche sous chargements sinusoïdaux et sismiques

J. Pérez-Herreros & F. Cuira
Terrasol (SETEC group), Paris, France

S. Escoffier
IFSTTAR, GERS, SV, Nantes, France

P. Kotronis
Ecole Centrale de Nantes, Université de Nantes, CNRS, GeM, Nantes, France

ABSTRACT: An experimental centrifuge study is presented on the dynamic response of a pile group in a multilayered soil subjected to a series of sinusoidal and earthquake loadings. The foundation consists of a group of five end-bearing piles that support two different structures. The soil profile is composed of three horizontal layers alternating dense HN31 sand (bottom and top layers) and overconsolidated Speswhite kaolinite. The reproducibility of the soil foundation is verified using bender element measurements. The dynamic responses of the piles are analyzed in terms of maximum bending moments and compared to the results obtained for a single pile subjected to kinematic interaction.

RÉSUMÉ: L'étude expérimentale en centrifugeuse d'un groupe de pieux dans un sol multicouche soumis à une série de chargements sinusoïdaux et sismiques est présentée. La fondation consiste en un groupe de cinq pieux encastrés en pointe supportant deux structures différentes. Le profil de sol est composé de trois couches horizontales alternant du sable dense HN31 (couches inférieure et supérieure) et de la kaolinite Speswhite surconsolidée. La répétabilité du massif de sol est vérifiée à partir de mesures avec des bender elements. Les réponses dynamiques des pieux sont analysées en termes de moment de flexion maximal et comparées à la réponse d'un pieu isolé sous chargement cinématique.

Keywords: centrifuge; soil-structure interaction; multilayer soil profile; pile group; earthquake loading

1 INTRODUCTION

The dynamic response of a structure supported by a pile-group foundation is a complex Soil-Structure Interaction problem. Nevertheless, few experimental studies exist on the behavior of pile groups in clay and stratified soils under seismic loading (Meymand 1998, Wilson 1998, Boulanger *et al*. 1999, Banerjee 2009, Zhang *et al*. 2017, Taghavi *et al*. 2017).

A series of experimental centrifuge tests on end-bearing single piles and pile groups in a stratified soil profile is conducted to increase the existing databases and to validate numerical models. In order to understand the mechanisms of soil-pile interaction in the case of pile groups,

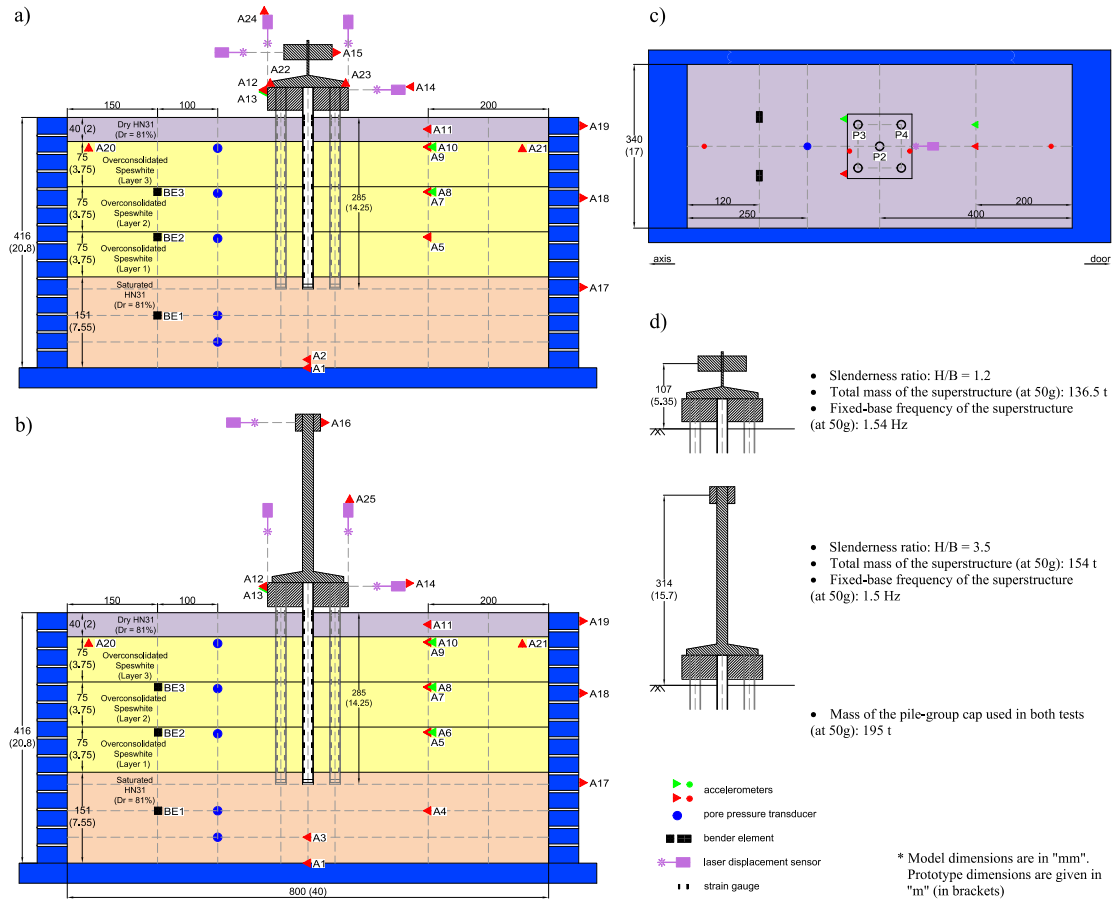

Figure 1. Experimental layout: a) C07 test with a short superstructure; b) C08 test with a tall superstructure; c) top view of C07 and C08 tests; and d) characteristics of the superstructures.

two tests were performed on a pile group of five piles supporting two different superstructures (a short and a tall one). The present article focuses on the results of these two tests.

2 EXPERIMENTAL SETUP AND PROCEDURE

The tests are performed in an ESB (Equivalent Shear Beam) container at 50g using the 5.5 m radius centrifuge at IFSTTAR (Corté & Garnier 1986). A complete introduction along with the scaling factors commonly used in centrifuge modeling is given for example in Garnier (2001). Figure 1 depicts the layout of the pile group tests identified as C07 and C08.

The soil profile consists of three horizontal layers of saturated Hostun HN31 sand (bottom), overconsolidated Speswhite kaolin clay (middle) and dry Hostun HN31 sand (top). The properties of clay and sand are summarized in Tables 1 and 2.

The sand layers are obtained by air pluviation with an automatic hopper system at 1g (Ternet 1999). The relative density is controlled to be 81%. The sand layer at the bottom of the container is vacuum saturated with water to avoid desaturation at the bottom of the clay layer and liquefaction of the sand layer (due to scaling laws the simulated prototype has a higher per-

Table 1. Properties of Speswhite kaolin clay (Khemakhem 2012)

Symbol	Material properties	Value
γ_s	Unit weight of the grains	26.5 kN/m^3
w_P	Plastic limit	30 %
w_L	Liquid limit	55 %
I_P	Plasticity index	25 %
C_c	Compression index	0.33
C_s	Recompression index	0.06

Table 2. Properties of Hostun HN31 sand (Benahmed 2001)

Symbol	Material properties	Value
d_{50}	Average grain size	0.35 mm
C_u	Coefficient of uniformity	1.57
e_{min}	Minimum void ratio	0.656
e_{max}	Maximum void ratio	1
γ_s	Unit weight of the grains	26 kN/m^3
$\gamma_{d,min}$	Minimum dry unit weight	13.047 kN/m^3
$\gamma_{d,max}$	Maximum dry unit weight	15.696 kN/m^3

meability). The overconsolidated speswhite kaolinite formation is prepared in three layers. Each layer is consolidated up to 160 kPa preloading pressure at 1g. The OCR values in the middle of the layers 1, 2 and 3 (Figs. 1a and 1b) are 1.55, 2.13 and 3.42 respectively. Finally, the top dry sand layer is air-pluviated above the overconsolidated clay layer.

The soil profile is subjected to four 1g-50g-1g cycles followed by a stabilization phase at 50g prior to the application of dynamic loads (based on the work of Khemakhem 2012).

The soil model is instrumented with accelerometers, pore pressure sensors and bender elements (Fig. 1). The last ones are used to compare the shear wave velocity at different levels between both containers. The results are discussed in the following section. In addition, the response of the superstructure is recorded with accelerometers and laser sensors. Due to the article size limitations, pore pressure and displacement measurements are not discussed hereafter.

The group of piles consists of five tubular aluminum piles with a minimum distance between axes of 3.54 diameters (tradeoff between

Table 3. Properties of the piles

Property	Hollow aluminum (model scale)	Reinforced concrete (prototype scale)
Outer diameter	18 mm	0.977 m
Length	335 mm	16.75 m
Young modulus	74 GPa	20 GPa
Flexural rigidity	1.43E-04 MNm²	8.95E02 MNm²
Yield moment	5.27E-05 MNm	6.59 MNm

Table 4. Characteristics of the reference signals (prototype scale)

#	Input	PGA (g)	PGV (m/s)	Ia (m/s)	Duration (s)
1	Northridge	0.05	0.037	0.025	11.163
2	Landers	0.05	0.051	0.031	11.505
3	Northridge	0.3	0.220	0.897	11.163
4	Landers	0.3	0.306	1.109	11.505
5	Sine 1 Hz	0.1	0.157	1.417	16.348
6	Sine 3.2 Hz	0.1	0.049	0.443	5.112
7	Sine 1.8 Hz	0.1	0.087	0.787	9.089
8	Sine 2.4 Hz	0.1	0.065	0.588	6.808
9	Sine 3.2 Hz	0.3	0.146	3.986	5.112
10	Sine 1.8 Hz	0.3	0.261	7.087	9.089
11	Sine 2.4 Hz	0.3	0.195	5.295	6.808
12	Northridge	0.05	0.037	0.025	11.163
13	Landers	0.05	0.051	0.031	11.505

center-to-center separation of piles and the distance of the outer piles to the container to limit boundary effects). The layout and the distribution of the piles are indicated in Figure 1. Three of the piles are instrumented with 14 equally spaced half-bridge strain gauges along the inner side of the pile shaft in order to calculate the bending moment distribution. The uppermost strain gauges are located at the soil surface level. The properties of the piles are given in Table 3.

The pile group is installed at 1g using a hydraulic actuator. A low driving speed of 0.1 mm/s is used to allow dissipation of pore pressure in the surrounding soil. The pile tip is embedded one diameter in the saturated sand layer. To avoid soil-cap interaction, the pile cap is kept at a distance of 12 mm above the ground surface (0.6 m at prototype scale).

Two different superstructures are used in the tests with a measured fixed-base frequency re-

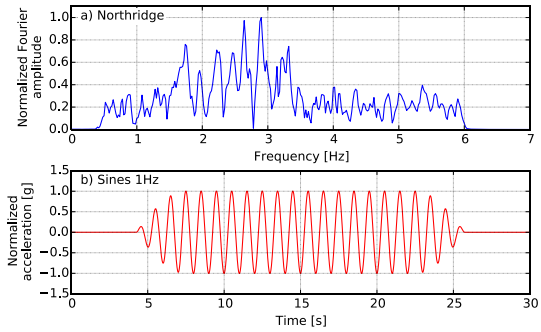

Figure 2. Frequency and time representation of the Northridge earthquake and 1 Hz sine input (prototype scale)

sponse at 50g of 1.54 Hz and 1.5 Hz for the short and the tall superstructure, respectively (Fig. 1d). The main difference between the superstructures is the slenderness ratio which is almost 3 times higher in the case of the C08 test.

Each container has been subjected to 13 successive base shakings. Between each base shaking a sufficient time for pore pressure dissipation has been respected. Two types of inputs are used: sines with tapered parts and real broadband earthquakes (Landers 1992 (Lucern Valley station) and Northridge 1994 (Tarzana station) records). Earthquake signals have been filtered outside the frequency range of 0.4-6 Hz in order to be in the capacity range of the shaker (Chazelas *et al*. 2008). The characteristics of the reference signals are given in Table 4 (PGA and PGV: peak ground acceleration and velocity, Ia: Arias Intensity).

3 ANALYSIS OF THE RESULTS

Unless otherwise indicated, the experimental results are given using prototype scale units.

3.1 Shear wave velocity profile

The shear wave velocity is calculated from bender element measurements performed just before the first base shaking at several depths (6 m, 9.75 m and 15.6 m). The results are compared to a theoretical profile estimated using

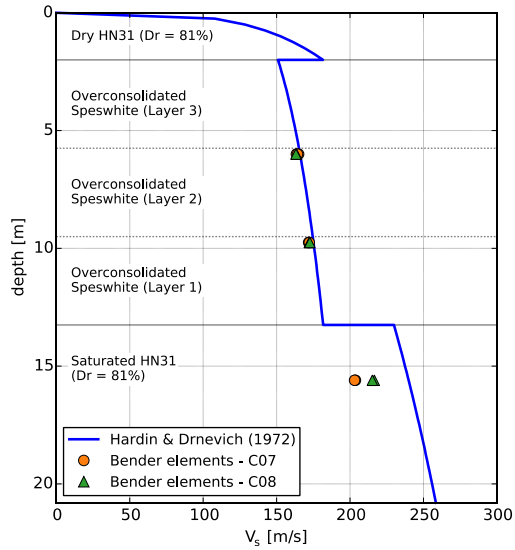

Figure 3. Small-strain shear wave velocity measures estimated from bender element tests compared to the Hardin & Drnevich (1972) empirical formulation.

the empirical expression proposed by Hardin & Drnevich (1972) in Fig. 3.

A good reproducibility in terms of shear wave velocity is observed for the C07 and C08 tests in the clay layer, with a maximum variation of 0.6% between both tests. In the case of the saturated sand layer a difference of 6.2% is found. The small deviations observed suggest a good reproducibility of the shear wave velocity in the initial state.

In addition, a good agreement between experimental results and the theoretical expression is found, specially for the clay layer.

3.2 Evolution of bending moment with time

Figures 4 and 5 show the time evolution of the normalized bending moment in piles and the envelope of maximum bending moment for the 1Hz 0.1g PGA sine input and the 0.3g PGA Northridge earthquake. Only the part of the bending moment response induced by each solicitation is considered in this analysis: the offset at the beginning of each input has been removed and the cumulated residual moment is therefore not present in the maximum moment envelopes.

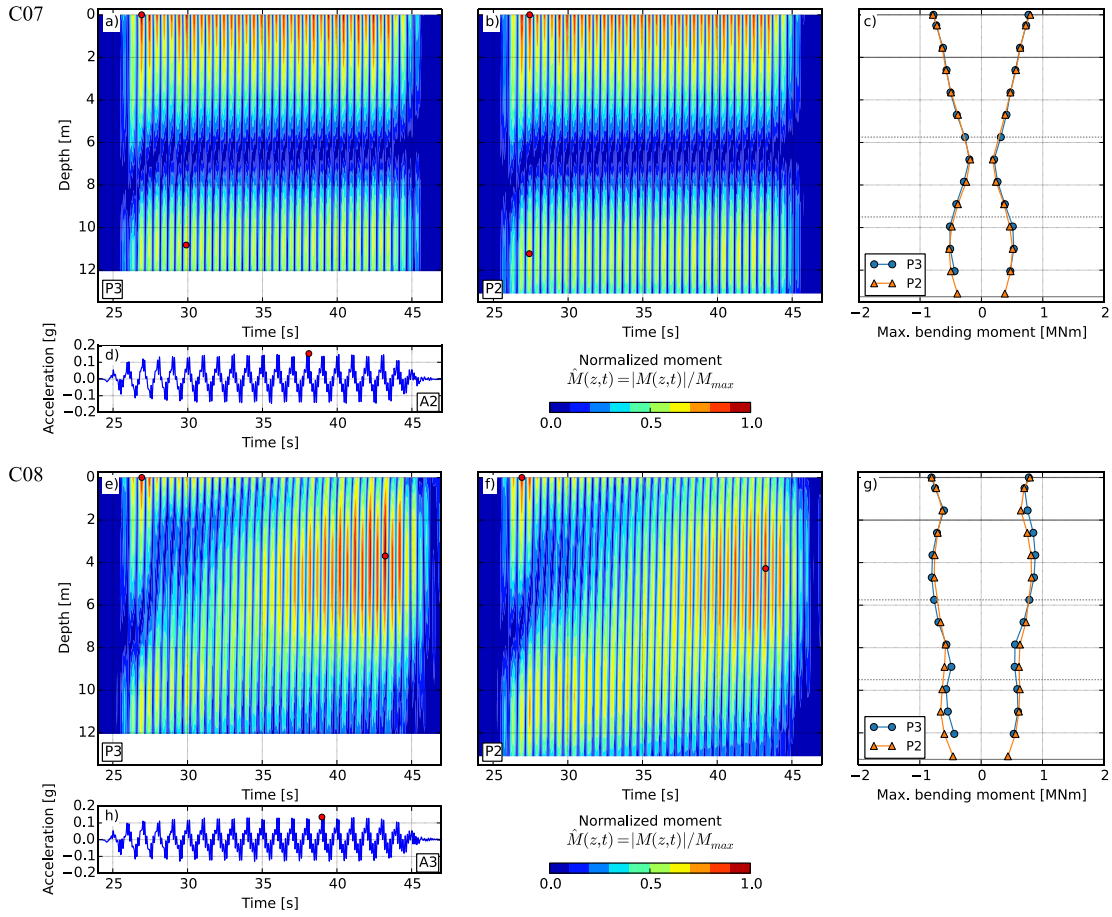

Figure 4. Time evolution of the normalized bending moment and envelope of the maximum bending moment in piles for Sine 1Hz 0.1g input: a-d) results from C07 test and (e-h) from C08 test.

Results are given for two instrumented piles in the group, the P2 pile in the center and the P3 pile in the outer part of the pile group (Fig. 1c). To improve visibility, the moment history is normalized with the maximum bending moment recorded in both piles. The acceleration recorded in the dense sand layer under the pile group (at a depth of 19.55 m and 18.05 m in the case of C07 and C08 tests respectively) is also given for comparison.

The main observation is that the maximum bending moment at different parts of the piles is not reached at the same time.

The maximum bending moment in the upper part of the pile is reached at the level of the ground surface for the two inputs and the two tests. For the case of the Northridge earthquake and for both containers, it is reached just after the maximum acceleration has been recorded at the bottom of the soil profile.

Regarding the maximum bending moment in the lower part of the pile, the response of both tests is similar during the first cycles of the Sine 1Hz input. After the first four cycles of the C07 test, the maximum moment profile stabilizes. In the lower part of the pile, the maximum moment remains stable both in value (maximum value of 0.53 MNm recorded in P3 pile) and in depth (around 11 m). In the case of the C08 test with the slender superstructure however, there is a

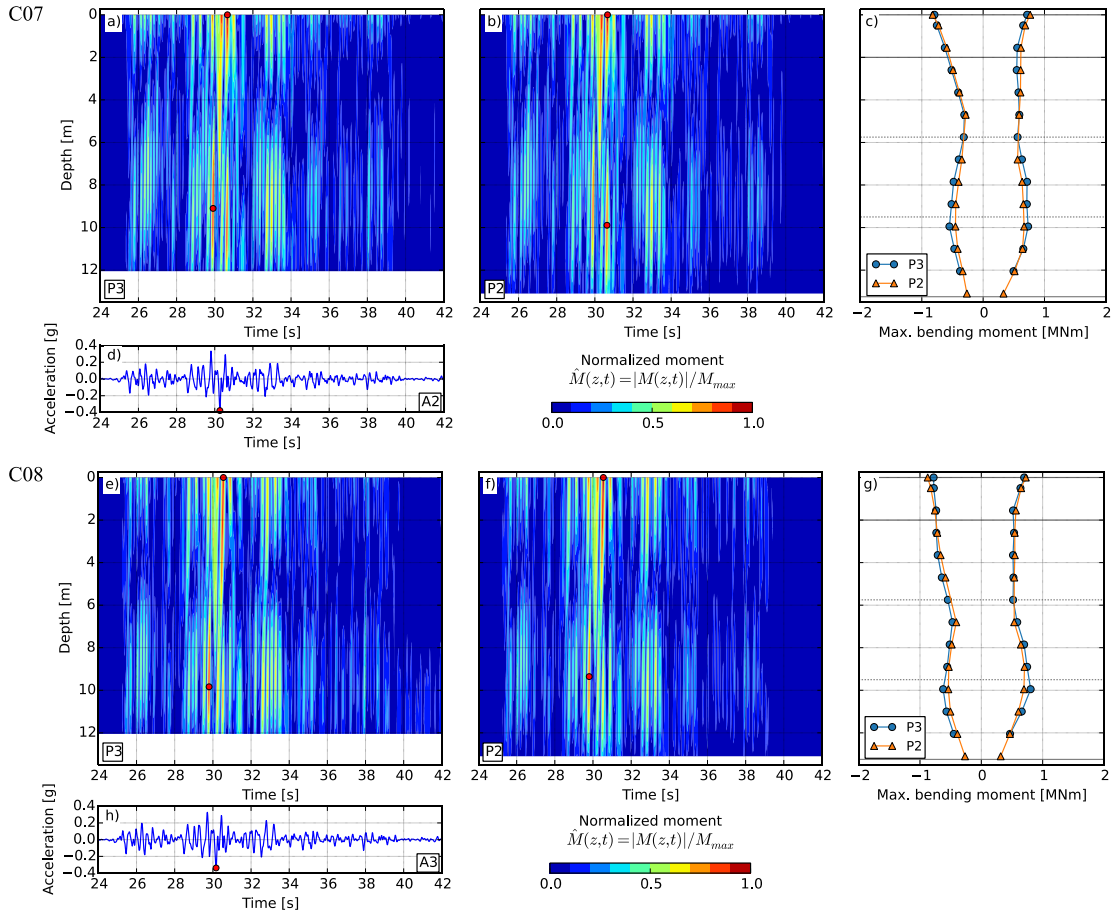

Figure 5. Time evolution of the normalized bending moment and envelope of the maximum bending moment in piles for Northridge 0.3g earthquake: (a-d) results from C07 test and (e-h) from C08 test.

sharp evolution of the moment profile over time. The maximum moment that is initially recorded in the lower part of the pile evolves in amplitude with the cycles. The depth at which the maximum bending moment is recorded also changes with the cycles, from a depth of about 11 m to 4 m when the maximum moment is recorded (0.88 MNm in P3 pile). Fig. 6 shows the evolution of the envelope of maximum bending moment in P2 for different time ranges. This evolution indicates an important modification of the response of the sol-pile-superstructure system with time.

In the case of the strong Northridge earthquake, the bending moments are found similar for both tests with slight differences recorded around 4 m depth, directly influenced therefore by the pile head conditions. The maximum bending moment in the lower part of the pile is not negligible compared to the maximum bending moment recorded at the soil surface. It is located at a depth of about 9.4 m, with a little variation from pile to pile and between tests (±0.4 m).

From these results it can be concluded that the response of the system in terms of maximum bending moment depends on the type of loading, its intensity and frequency content but also the characteristics of the superstructure which in this case is essentially the slenderness ratio. The

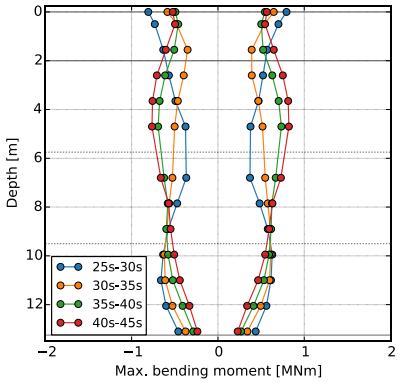

Figure 6. Maximum bending moment envelopes at different time periods for C08 test and Sine 1Hz 0.1g input.

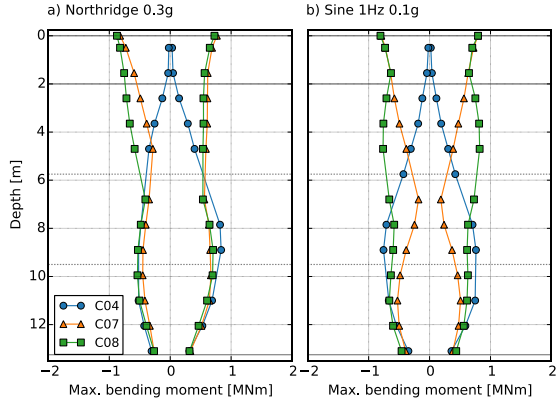

Figure 7. Maximum bending moments: results from the single pile test (C04) vs the pile group tests (C07 and C08).

difference in the response between C07 and C08 tests for the 1Hz Sine signal is related to the difference in terms of slenderness ratio between the two superstructures and therefore the presence of a higher rotational component in the response of C08 test that amplifies the response of the piles in their upper part and influences the reaction of the surrounding soil.

For the case of the Northridge earthquake, the frequency content of the applied signal is the reason behind the similar results obtained for both tests. In contrast to the Sine 1Hz signal, the Northridge earthquake signal energy is concentrated in the frequency range from 1.5Hz to 3.5Hz, whereas the response frequency of the soil column has been estimated close to 1Hz for the 0.3g PGA Northridge earthquake. The loading frequency being relatively far from the fundamental response of the soil column and of the soil-structure system, amplification effects are less important.

3.3 Inertial vs kinematic interaction

The maximum bending moment envelopes recorded in both tests for the P2 pile (center pile) are compared in Fig. 7 to the envelopes from the C04 test, consisted of a single pile without mass at the pile head in the same soil profile and subjected to the same inputs (Pérez-Herreros *et al.* 2018). This comparison is a first attempt to analyze the importance of the kinematic and inertial interaction effects on the bending moment profile pile response.

In the case of the Northridge earthquake, the same shape of maximum bending moment profile is found from the pile tip to a depth of about 7 m. Therefore, the response in this part of the pile is esentially controlled by the kinematic interaction due to the embedment of the piles of a diameter in the dense sand layer at the bottom of the soil profle. The response at the upper part of the piles is influenced by inertial interaction effects.

Concerning the Sine 1Hz input, a close response is found for the three tests only from a depth beyond 11 m. This indicates that inertial interaction effects play an important role in the pile response in the first 11 m.

This comparison helps to better understand the results presented in the previous paragraphs regarding the time evolution of the bending moments, especially for the case of the 1Hz Sine input in the C08 test.

The response of the system for that particular case can be explained by the interaction between the kinematic and inertial effects. The amplitude of the response in the upper part of the piles degrades the surrounding soil and thus the soil reaction. The decrease of the soil reaction is accompanied with an increase of the

displacements, the rotations and the bending moment in the upper part of the pile which, as already observed, is essentially controlled by the inertial loadings at the pile head. At the same time, the diminution of the reaction in the upper part of the pile has an influence on the kinematic origin bending moment. The soil reaction in the upper part of the pile being smaller, the pile is able to better accommodate kinematic deformations induced by the pile tip embedment in the dense sand layer at the bottom of the soil profile. As a consequence, the bending moment in the lower part of the pile is reduced as shown in Fig. 6.

It can be concluded that the interactions of inertial or kinematic origin can be brought to interact together and may result in a complex evolution of the response of the system with time under certain configurations.

4 CONCLUSIONS

Dynamic centrifuge tests were conducted to study the behavior of end-bearing pile groups in a layered soil supporting two different superstructures. The following first conclusions are drawn:

- Despite the complexity in the fabrication of the soil profile, the differences between the two tests in terms of shear wave velocity remain below 6.2%, which proves a satisfactory repeatability of the soil profile.
- The maximum bending moments in different parts of the pile are not reached at the same time during the loading.
- The response of the system in terms of maximum bending moment depends on the type of loading, the intensity, the frequency content and the conditions at the pile head.
- The interactions of inertial or kinematic origin can be brought to interact together and may result in a complex evolution of the response of the system under certain configurations.

5 REFERENCES

Banerjee, S. 2009. Centrifuge and numerical modelling of soft clay-pile-raft foundations subjected to seismic shaking. Ph.D. thesis, National University of Singapore.

Benahmed, N. 2001. Comportement mécanique d'un sable sous cisaillement monotone et cyclique. Ph.D. thesis, Ecole Nationale des Ponts et Chaussées.

Boulanger, R.W., Curras, C.J., Kutter, B.L., Wilson, D.W. & Abghari, A. 1999. Seismic soil-pile-structure interaction experiments and analyses. J. Geotech. Geoenviron. Eng., 125, 750-759.

Chazelas, J.L., Escoffier, S., Garnier, J., Thorel, L. & Rault, G. 2008. Original technologies for proven performances for the new LCPC earthquake simulator. Bull. Earthquake Eng., 6: 723-728.

Corté, J. & Garnier, J. 1986. A centrifuge for research in geotechnics. Bulletin Liaison Laboratoire Ponts et Chaussées, 128.

Garnier, J. 2001. Modèles physiques en géotechnique: Etat des connaissances et avancées récentes. Première Conférence Coulomb, CFMS.

Khemakhem, M. 2012. Etude experimentale de la response aux charges laterales monotones et cycliques d'un pieu fore dans l'argile. Ph.D. thesis, Ecole Centrale de Nantes.

Meymand, P.J. 1998. Shaking table scale model tests of non-linear soil-pile-superstructure interaction in soft clay. Ph.D. thesis, University of California, Berkeley.

Pérez-Herreros, J., Escoffier, S., Kotronis, P. & Cuira, F. 2018. Kinematic interaction of piles under seismic loading. 9th ICPMG, London.

Taghavi, A., Muraleetharan, K.K. & Miller, G.A. 2017. Nonlinear seismic behavior of pile groups in cement-improved soft clay. Soil Dyn. Earthquake Eng. 99, 189-202.

Ternet, O. 1999. Reconstitution and characterization of the sand samples. Application to the tests out of the centrifuge and calibration chamber. Ph.D. thesis, Université de Caen.

Wilson, D.W. 1998. Soil-pile-superstructure interaction in liquefying sand and soft clay. Ph.D. thesis, University of California, Davis.

Zhang, L., Goh, S.H. & Yi, J. 2017. A centrifuge study of the seismic response of pile - raft systems embedded in soft clay. Géotechnique, 67, 479-490.